Effect of orifice configuration on the penetration height in crossflow

Jun Hee Kim*, Kun Woo Ku*, Hyun Jin Youn*, Jung Goo Hong*†,
Choong Won Lee* and Kyung Yul Chung**

* Department of Mechanical Engineering
Kyungpook National University
1370 Sankyuk-dong Buk-gu, Daegu, Republic of Korea

** Environment and Energy Systems Research Division
Korea Institute of Machinery and Materials
104 Sinseongno, Yuseong-gu, Daejeon, Republic of Korea

Abstract

In previous researches on jet in crossflow (JICF), which is applied for the liquid jet injection system of air-breathing propulsion systems or rocket engine system, more than 20 different correlations of jet penetration have been proposed. In these proposed correlations, the relationships between jet penetration and the various flow parameters (momentum flux ratio, Reynolds number, Weber number, viscosity ratio, etc.) were defined. But, most of these studies were carried out using the single orifice injector (SOI). In this study, in order to define the interference effects of liquid jet penetration in crossflow, the double orifice injector (DOI) is adopted. First, the jet penetration correlation of SOI according to the crossflow temperature controlled by the vitiated air heater is proposed. The jet penetration height for heated crossflow is lower than that for cold crossflow because of the increase of crossflow velocity despite the lower density. The jet penetration correlation of DOI is derived for variations of injector orifice spacing. In the case of the DOI, since the front liquid jet acts as a shield of the rear liquid jet, the jet penetration with DOI is higher than that with SOI. With the double orifice injector, the rear jet penetration height is increased as the nozzle spacing is decreased. And, The penetration height correlation for the rear liquid jet with DOI was developed. As the nozzle spacing increases, the jet penetration height decreases; therefore, an inverse relationship between nozzle spacing and jet penetration height is expected.

Introduction

In a liquid fuel injection system, the jet in crossflow (JICF), which injects perpendicularly into the crossflow, is a common strategy for improving fuel/air mixing in a propulsion system.[1] JICF is widely used in engineering systems such as air-breathing engines (dilution air jets, fuel/air mixer, turbine blade film cooling systems, ramjet/scramjet fuel injector) and a rocket engine system (vector thrust control).[2] For high speed air-breathing engines such as a ramjet/scramjet, the JICF injection system provides good mixing performance. [3-5]

Early review of the behavior of JICF was presented by Schetz et al.[6] and Nejad et al.[7] In addition to important parameters such as liquid breakup, penetration height, droplet size, droplet velocity and liquid volume flux distribution need to be considered for cross flow evaluation, the penetration height of the liquid jet is important parameters that indicates how well the injected liquid mixes with the free-stream air.[8] Schetz et al.[6] concluded that the injected liquid breaks up because of large amplitude surface waves, and that the jet column fraction location increases with the increase in jet-to-air momentum flux ratio. Wu et al.[9,10] proposed the breakup map and the relations of penetration height, spray width and cross-sectional area with jet-to-air momentum flux ratio, respectively. Power-law correlations were developed by Wu et al.[9], Lin et al.[11], Iyogun el al.[12], Ragucci et al.[13], Bellofiore et al.[14], Birouk et al.[15], Masuda and McDonell[16], Stenzler et al.[17] and Elshamy and Jeng[18], etc. The basic form of power-law correlations is as follows;

$$\frac{Y}{d} = A \cdot q^B \cdot \left(\frac{X}{d}\right)^C \qquad (1)$$

In the power-law correlation, the jet penetration (Y/d) is a function of the jet-to-air momentum flux ratio (q) according to the parameter considered in the correlations such as Weber number, viscosity ratio, Reynolds

†Corresponding author: jghong70@knu.ac.kr

number, pressure ratio [19]. Wu et al.[9] presented correlations for the column regime and droplet regime, respectively. Ragucci et al.[13], and Masuda and McDonell[16] presented correlations that included Weber number and viscosity ratio. In particular, Stenzler et al.[17] presented correlations for heated and unheated crossflows. But, with the exception of q, other parameters, such as Weber number, viscosity ratio, Reynolds number, pressure ratio, do significantly impact the penetration height.

Logarithmic correlations were proposed by Inamura et al.[20], Becker and Hassa [21,22], and Lakhamraju and Jeng[23], etc. The basic form of the logarithmic correlations is as follows;

$$\frac{Y}{d} = A \cdot q^B \cdot \ln\left(1 + C \cdot \frac{X}{d}\right) \qquad (2)$$

The jet penetration (Y/d) is a function of q, but independent of Weber number, and the viscosity ratio. As in other previous studies, increasing the Weber number decreased the average droplet size and since smaller droplets decelerate faster, the overall penetration height of the spray decreased.[24] However, the influence of Weber number is insignificant.

In JICF systems, penetration height (fuel/air mixing performance) is generally controlled by adjusting q.[25,26] Effective control and prediction methods of jet penetration height have been proposed. Lee et al.[25] proposed a JICF system with a protruding nozzle tip to effectively increase the mixing performance in JICF and to stabilize the combustion of ramjet combustor. However, the injection of multiple parallel jets in JICF has yet to be studied. Consequently, we present the main results on the interaction between multiple jets (double liquid jets) in crossflow. In our study, to increase the jet penetration height and to improve the mixing performance of JICF, multiple (double) liquid jets are used. a double liquid jet injector has two orifices in the direction of crossflow. The double liquid jet injector is used to study the jet penetration affected by the interaction between front orifice and a rear orifice.

Also, in the existing correlations of penetration height, various parameters were adopted: q, Weber number, viscosity ratio, Reynolds number, and pressure ratio. However, previous works except for Stenzler et al.[17] and Lakhamraju and Jeng[23] were conducted for cold flow conditions. In an actual ramjet engine, the temperature of the air induced into the combustor is more than 500K. Therefore, in our studies, to meet the actual crossflow temperature, the air was heated by a vitiated air heater (VAH) utilized to control the temperature and velocity of the air.[25]

The objective of this study is to present a set of penetration heights for double liquid jets injected into crossflow and to describe the influence of the double liquid jets. Thus, the jet penetration height correlation for the single liquid jet injector and double liquid jet injector is determined.

Experimental Methods

The penetration heights of a double liquid jet and a single liquid jet in JICF were studied by using a liquid ramjet experimental facility. A schematic diagram of the experimental apparatus is illustrated in FIG. 1. The experimental facility consisted of an elevated ambient pressure supply system, vitiated air heater (VAH), test section, and the pressure and flow rate measurement section. The elevated ambient pressure supply system consisted of a higher-capacity compressor, an air dryer, an air storage tank and a pressure control valve. In this study, the same air conditions as in a real flight, were set by the vitiated air heater (VAH).

The test section had a height of 100mm and a width of 100mm. The visualization windows, made of tempered glass, were installed on 2 sides of the test section, and 1 on the top. In order to maintain constant quantity of crossflow, a sonic nozzle was installed in front of the test section, and to measure and control the pressure of the test section, a pressure regulating valve and an orifice were used. The pressure and flow-rate measurement section were composed of a pressure sensor, data acquisition board, and micro-manometer. Also, the liquid jet penetrations in the JICF were analyzed by the shadowgraph method using a high-speed digital camera and a stroboscope. The shadowgraphs of the liquid jet were taken with Canon EF 50mm f/1.8 lens, and were synchronized with the digital Camera (Canon EOS 20D) and the stroboscope. In this study, 20 instantaneous images were taken for each test condition. The original images were taken image processing such as background subtraction, histogram equalization, and thresholding using self-developed image-processing program.

FIG. 2 shows the test section and injector shape. The single orifice injector (SOI) and double orifice injector (DOI) were adopted. Especially, the double orifice injector was used to study the increase in jet penetration due to the interaction between the liquid jets. The specifications of the injectors are tabulated in Table 1.

The experimental test conditions are tabulated in the Table 2.

In JICF, due to its interaction with the crossflow and, for the case of the flush jet in the crossflow, the spray and atomization pattern is a more complicated than that of a free jet in quiescent surroundings.[2]

In this study, the momentum flux ratio and the Weber number were computed for both jet combined (not the rear jet only), and the effect of Weber number was not taken into account to evaluate the jet penetration height of

JICF. Also, in this study, the jet-to-air momentum flux ratio (q) and the mass flowrates of SOI and DOI were adjusted to be the same to identify the increased penetration height of the DOI under same flowfield conditions.

Results and Discussion

1. Single orifice injector

In FIG. 3, the jet penetration height of SOI is shown with the variation of the jet-to-air momentum flux ratio (q). The momentum flux ratio (q) is induced from the different temperature and pressure conditions with the cold flow conditions. In the test conditions, as the jet-to-air momentum flux ratio (q) and liquid jet velocity increased, the jet penetration height increased. At, v_j=2.9m/s, the liquid column was smooth immediately after injection. As v_j increases, droplets were generated by the waves on the leeward side of the liquid column, and the jet penetration increased. These results were in agreement with the results of other researchers.

In FIG. 7, the power-law correlation revealed the best-fit results of jet penetration height, unheated crossflow, all conditions crossflow, and heated crossflow. In Eq. (1), parameters A, B and C were determined independent of the error information provided by NLREG (Nonlinear Regression and Curve Fitting), and the model with the least average deviation was chosen. Eq. (1) after regression analysis yielded Eqs. (3), (4) and (5) with an average deviation of 1.68, 1.72 and 1.91, and coefficient of determination R^2=94.4%, 93.6% and 91.8%, respectively.

$$\frac{Y}{d} = 2.291 \cdot q^{0.417} \cdot \left(\frac{X}{d}\right)^{0.429} \quad \text{: unheated crossflow of SOI} \quad (3)$$

$$\frac{Y}{d} = 2.267 \cdot q^{0.409} \cdot \left(\frac{X}{d}\right)^{0.421} \quad \text{: all conditions of SOI} \quad (4)$$

$$\frac{Y}{d} = 2.241 \cdot q^{0.402} \cdot \left(\frac{X}{d}\right)^{0.410} \quad \text{: heated crossflow of SOI} \quad (5)$$

The jet penetration heights of unheated crossflow were slightly higher than the jet penetration heights of all heated crossflow conditions. When the temperature of the crossflow increased, jet penetration was allowed the contradictory impact. First, jet penetration was increased because of the reduced density of the crossflow as the temperature rose. On the other hand, the jet penetration was reduced because of the increase of crossflow velocity to meet the same the jet-to-air momentum flux ratio (q). In the case of the heated crossflow, the increased crossflow velocity had a greater impact on the jet penetration height than the reduced density of the crossflow did. These results were consistent with the correlation of Lakhamraju et al.[23], in which the increase in airstream temperature resulted in decreases in liquid jet penetrations. In Eq. (6), derived by Lakhamraju et al.[23], jet penetration is only slightly negatively dependent on crossflow temperature.

$$\frac{y}{d} = 1.844 \cdot q^{0.456} \cdot \ln\left(1 + 1.324 \cdot \frac{x}{d}\right) \cdot \left(\frac{T_a}{T_{amb}}\right)^{-0.117} \quad \text{: Lakhamraju et al. [23]} \quad (6)$$

However, the temperatures of liquid jet and the crossflow were changed at the same time in the correlation of Lakhamraju et al.[23], whereas the temperature of crossflow was changed only in the present heated condition. Therefore, it can be identified the effect of increased velocity on jet penetration height between increased velocity and reduced density of heated crossflow.

FIG. 5 shows the penetration height calculated by various correlations of the basic power-law form at d=1mm, q=10 and We=13.7. The correlations of this study give similar results with those of Iyogun at al.[12] and Birouk et al.[15] In the comparison with Wu et al.[9] and Elshamy and Jeng [18], the discrepancies among the correlations are obvious. It may be due to the different injector geometry and different image processing method used, but the trend of penetration height according temperature are similar to those of Iyogun at al. (2006), Birouk et al. [15], Wu et al.[9], and Elshamy and Jeng [18]. So, many of these correlations are applicable to specific operation conditions, injector geometries and measurement techniques.

2. Double orifice injector

FIG. 6 is a 2-step threshold image of the typical spray pattern of DOI and the variation of jet penetration for q at L_h=4mm, obtained through image processing used to find the jet penetration height. The jet penetration height of the rear orifice rapidly increased at the intersection point with front liquid jet. In addition, the slope of the rear liquid jet, at the initial region of injection, was larger than that of the front liquid jet because of the reduction of the crossflow drag. As a result, since the front liquid jet acted as a shield of the rear liquid jet, the jet penetration of DOI was higher than that of SOI. Also, the jet penetration is increased, with increases of the jet-to-air momentum flux ratio (q), and liquid jet velocity (vj).

FIG. 7 shows the penetration height from the rear orifice of DOI according to nozzle spacing (L_h). At L_h= 4 (mm), the jet penetration height of DOI was much higher than that of SOI. The penetration height of the rear liquid jet was decreased as the nozzle spacing was increased. When the nozzle spacing was 12mm, the jet penetration from the rear orifice of DOI was as almost the same as the penetration height of SOI. These results were due to the reduction of crossflow drag at the rear liquid jet when nozzle spacing was decreased. However, as nozzle spacing was increased, the reduction of the crossflow drag disappeared. Eventually, in the case of DOI, the jet-to-air momentum flux ratio (q) and the nozzle spacing (L_h) became the major factors affecting penetration height. In addition, if L_h > 14mm, the penetration height is expected to hardly increase.

In FIG. 8, the correlation of the jet penetrations of the rear liquid jet of DOI is shown with the change of the nozzle spacing. The power-law correlation revealed that the best-fit results for the jet penetration heights, for L_h = 4, 8, 12 mm, were correlated with the average deviation of 1.84 and coefficient of determination R^2=94.4%. The modified correlation obtained is as follows:

$$\frac{Y}{d} = 3.060 \cdot q^{0.436} \cdot \left(\frac{X}{d}\right)^{0.445} \cdot \left(\frac{L_h}{d}\right)^{-0.175} \quad (7)$$

As stated earlier, to determine the influence of (L_h/d) on jet penetration height, the term (Lh/d)n was added to the equation. As the nozzle spacing (L_h) increased, the jet penetration height decreased, showing the inverse relationship between nozzle spacing and jet penetration height.

Summary and Conclusions

1. For the single orifice injector (SOI), three correlations of jet penetration height were developed,

$$\frac{Y}{d} = 2.291 \cdot q^{0.417} \cdot \left(\frac{X}{d}\right)^{0.429} \quad \text{: unheated crossflow of SOI} \quad (3)$$

$$\frac{Y}{d} = 2.267 \cdot q^{0.409} \cdot \left(\frac{X}{d}\right)^{0.421} \quad \text{: all conditions of SOI} \quad (4)$$

$$\frac{Y}{d} = 2.241 \cdot q^{0.402} \cdot \left(\frac{X}{d}\right)^{0.410} \quad \text{: heated crossflow of SOI} \quad (5)$$

2. For a heated crossflow, the jet penetration height was lower than that for a cold crossflow because of the increase of crossflow velocity, despite lower density

3. For the double orifice injector (DOI), the jet penetration height of the rear orifice jet rapidly increased at the intersection point with the front liquid jet. The slope of the rear liquid jet, at the initial region of injection, was greater than that of the front liquid jet because of lower crossflow drag. As a result, since the front liquid jet acted as a shield of the rear liquid jet, the jet penetration of DOI was higher than that of SOI. Also, the jet penetration is increased, as the jet-to-air momentum flux ratio (q), and liquid jet velocity (v_j) increased.

4. For the double orifice injector (DOI), the rear jet penetration height increased as the nozzle spacing decreased. The correlation of jet penetration height of the rear liquid jet of DOI was developed, and the modified correlation was obtained as follows:

$$\frac{Y}{d} = 3.060 \cdot q^{0.436} \cdot \left(\frac{X}{d}\right)^{0.445} \cdot \left(\frac{L_h}{d}\right)^{-0.175} \quad (7)$$

As the nozzle spacing (L_h) increased, the jet penetration height decreased, indicating an inverse relationship between nozzle spacing and jet penetration height.

Acknowledgements

This work was supported by Priority Research Centers Program through the National Research Foundation of Korea (NRF) funded by the Ministry of Education, Science and Technology (2011-0018392) and a part of the project titled "Development of TCS System on Green Ship Technology(20110153)" funded by the Ministry of Land, Transport and Maritime Affairs, Korea.

References

[1] Stenzler, J., Lee, J. G., and Santavicca, D. A., *Eastern States Section Meeting of the Combustion Institute*, pp.404-407, 2001.

[2] Karagozian, A.R., *Progress in Energy and Combustion Science*, vol. 36, pp.531-553, 2010.

[3] Abbitt, J. D., Segal, C., McDaniel, J. C., Krauss, R. H., and Whitehurst, R. B., *Journal of Propulsion and Power*, vol.9, no.3, pp.472-478, 1993.

[4] Wang, K. C., Smith, O. I., and Karagozian, A. R., *AIAA Journal*, vol.33, no.12, pp.2259-63, 1995.

[5] Curran, E. T., *Journal of Propulsion and Power*, vol.17, no.6, pp.1138-1148, 2001.
[6] Schetz, J. A., and Padhye, A., *AIAA Journal*, vol. 15, no. 10, pp.1385-1390, 1977.
[7] Nejad, A. S., and Schetz, J. A., *AIAA Journal*, Vol. 22, pp. 458, 459, 1984.
[8] Yoon, H. J., and No, S. Y., *ILASS-Asia 2011*, 2011.
[9] Wu, P. K., Kirkendall, K. A., and Fuller R. P., *Journal of Propulsion and Power*, vol.13, no.1, pp.64-73, 1997.
[10] Wu, P. K., Kirkendall, K. A., Fuller, R. P., and Nejad, A. S., *Journal of Propulsion and Power*, vol.14, no. 2, pp.173-182, 1998.
[11] Lin, K. C., Kennedy, P. J., and Jackson, T. A., *ILASS-Americas*, Madison, Wisconsin, pp.345-349, 2002.
[12] Iyogun, C. O., Birouk, M., and Popplewell, N., *Atomization and Sprays*, vol.16, pp.963-979, 2006.
[13] Ragucci, R., Bellofiore, A., and Cavaliere, A., *Proceedings of the Combustion Institute 31*, pp. 2231-2238, 2007.
[14] Bellofiore, A., Cavaliere, A., and Ragucci, R., *Combustion Science and Technology*, vol.179, pp. 319-342, 2007.
[15] Birouk, M., Iyogun, C. O., and Popplewell, N., *Atomization and Sprays*, vol.17, pp.267-287, 2007.
[16] Masuda, B. J., and McDonell, V. G., *Proc. ICLASS*, Kyoto, Japan, Paper ID ICLASS06-275, 2006.
[17] Stenzler, J. N., Lee, J. G., Santavicca, D. A., and Lee, W., *Atomization and Sprays*, vol.16, pp.887-906, 2006.
[18] Elshamy, O. M., and Jeng, S. M., *ILASS-Americas*, 2005.
[19] No, S. Y., *ILASS-Europe*, 2011.
[20] Inamura, T., Nagai, N., Hirai, T., and Asano, H., *Proc. ICLASS-91*, Gaithersburg, MD, USA, July, pp.839-846, 1991.
[21] Becker, J., and Hassa, C., *ILASS- Europe*, 1999.
[22] Becker, J., and Hassa, C., *Atomization and Sprays*, vol.11, pp.49-67, 2002.
[23] Lakhamraju, R. R., and Jeng, S. M., *ILASS-Americas*, Irvine, CA, May, 2005.
[24] Lubarsky, E., Shcherbik, O., Bibik, Y., Gopala, J. W., and Zinn, B. T., *ILASS-Americas*, 2011.
[25] Lee, C. W., Moon, S. Y., Sohn C. H., and Youn, H. J., *KSME Int'l Journal*, vol.17, no. 12, pp.2019-2026, 2003.
[26] Elshamy, O. M., Tambe, S. B., Cai, J., and Jeng, S.M., *45th AIAA Aerospace Sciences Meeting and Exhibit*, AIAA 2007-1370, 2007.

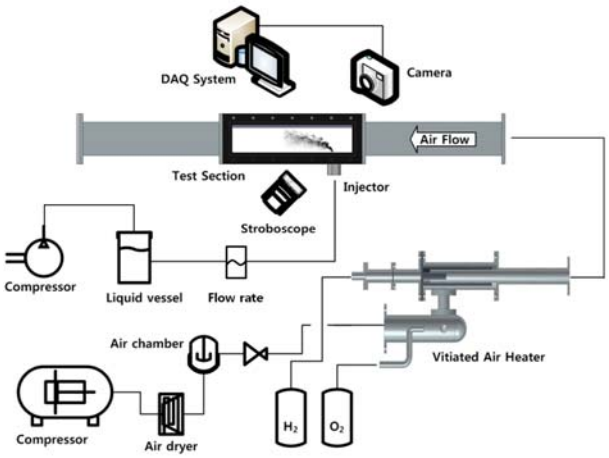

FIG. 1 Schematic diagram of experimental setup

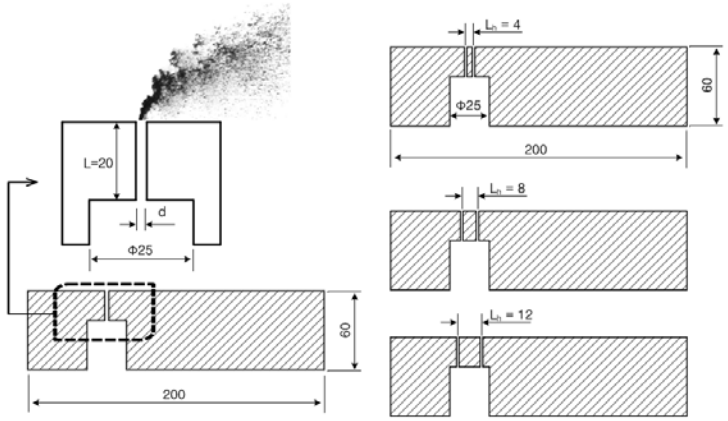

(a) Single orifice injector (SOI) (b) Double orifice injector (DOI)

FIG. 2 Injector shape

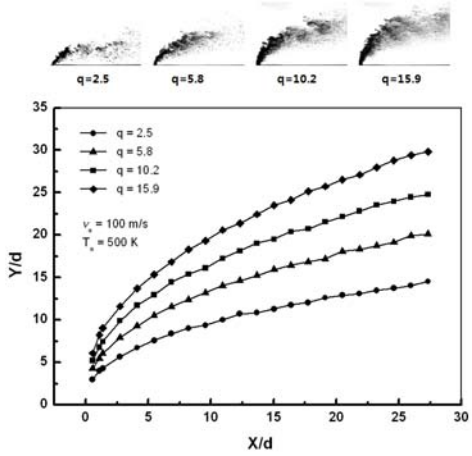

FIG. 3 Penetration height of SOI (v_a=100m/s, T_a=500K, d=1.0mm)

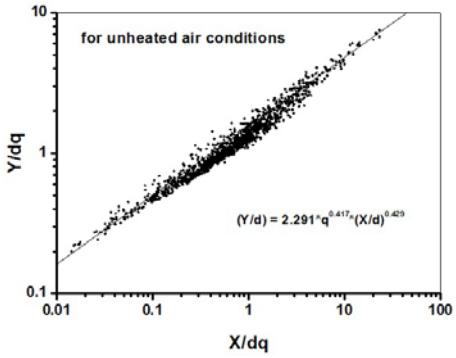

(a) Correlation of penetration height for unheated air conditions

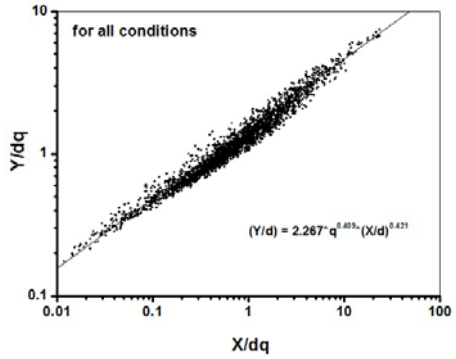

(b) Correlation of penetration height for all conditions

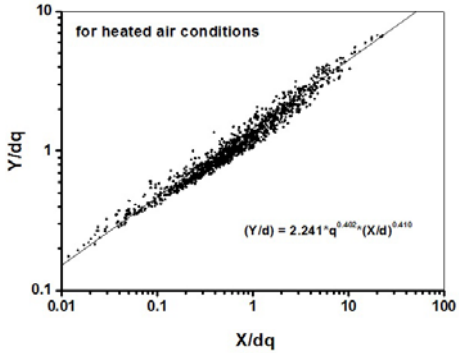

(c) Correlation of penetration height for heated air conditions

FIG. 4 Correlation of penetration height of SOI

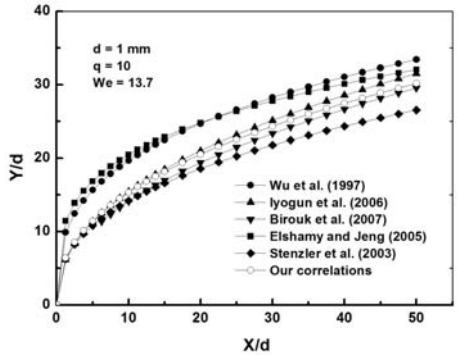

FIG. 5 Penetration heights with various correlations

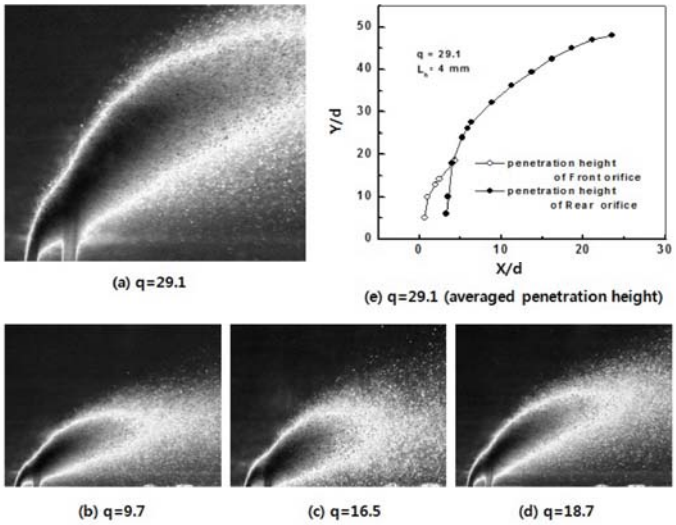

FIG. 6 Penetration height of DOI with various q. (L_h=4mm, T_a=293K)
: (a) q=29.1, (b) q=9.7, (c) q=16.5 and (d) q=18.7

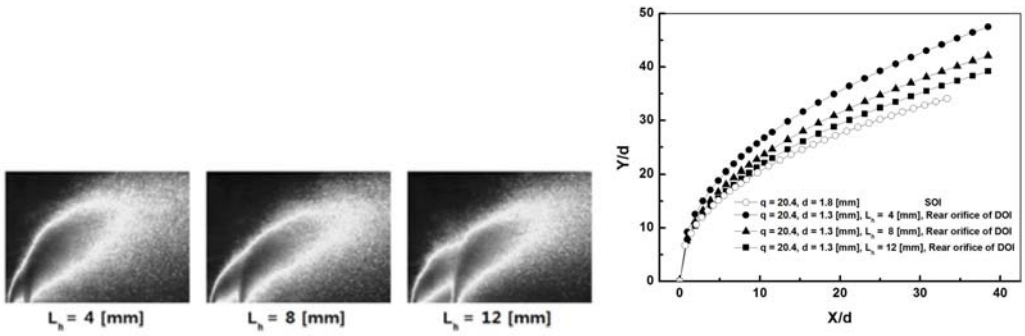

FIG. 7 Penetration height according to nozzle spacing in rear orifice of DOI (T_a=293K)

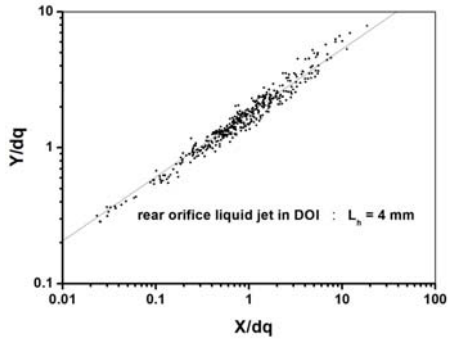

(a) Correlation of jet penetration (L_h = 4 mm)

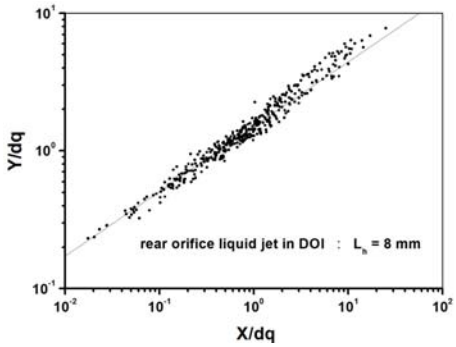

(b) Correlation of jet penetration (L_h = 8 mm)

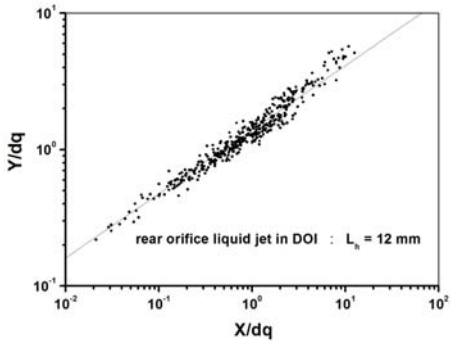

(c) Correlation of jet penetration (L_h = 12 mm)

FIG. 8 Correlation of penetration height in rear orifice jet of DOI

Table 1 Specification of injector

	Single orifice injector (SOI)	**Double orifice injector (DOI)**
d (mm)	1.0, 1.8, 2.1	1.3 × 2ea
L/d	> 10	> 10
L_h (mm)	-	4, 8, 12

Table 2 Experimental test conditions

Parameters		**Values**
Crossflow	Pressure [P_a]	1 ~ 5.1 (atm)
	Velocity [v_a]	40 ~ 100 (m/s)
	Temperature [T_a]	293, 500 (K)
	Viscosity [μ_a]	1.83×10^{-5} ~ 3.55×10^{-5} (N·s/m^2)
	Density [ρ_a]	1.19 ~ 0.457 (kg/m^3)
Liquid Jet	Fluid	Water
	Pressure [P_j]	2 ~ 8 (atm)
	Velocity [v_j]	3.3 ~ 9.6 (m/s)
	Temperature [T_j]	298 (K)
	Viscosity [μ_j]	1.0×10^{-3} (N·s/m^2)
	Density [ρ_j]	998 (kg/m^3)
	Surface tension [σ_j]	7.28×10^{-2} (N/m)
Jet-to-air momentum flux ratio (q)		2.0 ~ 29.1
Weber number (We)		5.3 ~ 47.9